VICTORIA UNIVERSITY

MELBOURNE AUSTRALIA

A Study of the Residual Strength of Reactive Powder-Based Geopolymer Concrete Under Elevated Temperatures

This is the Published version of the following publication

Article

A Study of the Residual Strength of Reactive Powder-Based Geopolymer Concrete under Elevated Temperatures

Thathsarani Kannangara *, Maurice Guerrieri, Sam Fragomeni and Paul Joseph

Institute for Sustainable Industries and Liveable Cities, Victoria University, P.O. Box 14428, Melbourne, VIC 8001, Australia; Maurice.Guerrieri@vu.edu.au (M.G.); sam.fragomeni@vu.edu.au (S.F.); Paul.Joseph@vu.edu.au (P.J.)
* Correspondence: a.kannangara@live.vu.edu.au

Abstract: This paper reports on studies relating to the unstressed residual compressive strengths of geopolymer pastes that are heated up to 800 °C, behavior of reactive powder concrete before and after exposure to elevated temperatures and thermal behavior of novel reactive powder geopolymer-based concretes. For this purpose, 10 geopolymer pastes and three reactive powder concrete mixtures were tested for residual strengths. Gladstone fly ash was used as the primary binder for both geopolymer pastes and reactive powder geopolymer concretes. In addition, four novel reactive powder geopolymer concrete mixes were prepared with zero cement utilization. While reactive powder concretes achieved the highest seven-day compressive strengths of approximately 140 MPa, very poor thermal behavior was observed, with explosive spalling occurring at a temperature of ca. 360 °C. The reactive powder geopolymer concretes, on the other hand, displayed relatively high thermal properties with no thermal cracking at 400 °C, or visible signs of spalling and very mild cracking in one case at 800 °C. In terms of the strength of reactive powder geopolymer concrete, a maximum compressive strength of approximately 76 MPa and residual strengths of approximately 61 MPa and 51 MPa at 400 °C and 800 °C, respectively, were observed.

Keywords: geopolymer; reactive powder; elevated temperatures; residual strength; spalling

1. Introduction

Owing to the increasing number of high fire risk infrastructures built around the world, including concrete tunnels, petrochemical plants, nuclear reactors, and oil refineries, concrete structures with a relatively high strength capacity and superior fire resistance are in high demand. Reactive powder concretes (RPC) were first developed in the early 1990s by a French Corporation [1]. They are currently used as an ultra-high performance concrete, where compressive strengths in the range of 150–800 MPa, tensile strengths between 6–13 MPa, flexural strengths in the range of 30–60 MPa and fracture energy in the range of 1200–40,000 J/m^2 can be achieved [1–4]. Related studies also reported that further enhancements in mechanical properties can be achieved through the reduction in the water to cement (w/c) ratio, exclusion of large aggregate particles, decrements in the calcium oxide to silicon dioxide ratio and through the addition of steel fibres as the reinforcement agent [5,6].

Typical dry ingredients of RPC include cement, as the binding material, together with silica fumes, an ultra-fine spherical shaped material, having an average diameter of about 0.15 μm and aggregate fillers, such as silica flour and fine sand/quartz particles, typically less than 600 μm in size [3,6]. The w/c ratio of RPC is reported to be between 0.1–0.25, whereas conventional concretes consist of a w/c ratio between 0.35–0.7 [6]. Superplasticizers (SP), which reduces the use of water whilst obtaining the required workability conditions, is considered as another key ingredient. A study on the influence of naphthalene, melamine and acrylic polymer superplasticizers on the strength and w/c ratio of RPC found that the incorporation of acrylic polymer superplasticizer generally required

a low w/c ratio [7]. Furthermore, specimens having the acrylic polymer superplasticizer recorded higher compressive strengths compared to the specimens that incorporated either of the other two ingredients.

In spite of its higher performance in terms of strength, RPCs behave very poorly in fire scenarios, where it often undergoes spalling, which is associated with the breaking away of concrete layers, thus causing degradation and loss of mechanical properties of the base matrix [8–12]. The compressive strength, tensile strength and fracture energy of RPCs when exposed to temperatures of up to 600 °C was investigated, where significant levels of spalling were also found to occur [8]. In addition, after being exposed to temperatures of 400 °C, the compressive strength was found to decrease significantly. It was also reported that the temperature range of 400–600 °C is the critical temperature range for spalling. When some similar properties were tested [11], the residual strength was found to vary, where it was found to decrease up to 100 °C, then increased over a temperature range of 200–500 °C and finally was observed to decrease above 600 °C. In addition, explosive spalling conditions were also found to occur during a temperature range of 260–520 °C.

On the other hand, geopolymer (GP) concretes, which is a mixture of a material(s) rich in silica and alumina, an alkaline liquid (most commonly a combination of sodium hydroxide, or potassium hydroxide and sodium silicate, or potassium silicate) and aggregate particles [13], have been reported to possess similar, if not better, performance as compared to conventional ordinary Portland cement (OPC)-based concretes, especially when exposed to heat/fire [14]. Reports also showed that GPs possess a relatively higher fire resistance owing to its ceramic-like properties and that GP composites are ideally suited for construction, transportation and infrastructure, where fire endurance is part of the requirements [15,16]. In addition to this, GP concretes were found to achieve high compressive strengths within 24 h of conditioning, provided an ease of workability and controllable setting times, possessed good abrasion resistance, superior resistance to alkali environments and exhibited low shrinkage and low thermal conductivity and high corrosion resistance for the steel reinforcement elements [17–21].

Türkmen et al. [22] investigated the residual compressive strength performance of 50 mm GP concrete cube specimens, having initial strengths of approximately 35 and 32 MPa, after being exposed to temperatures up to 700 °C. The average value over triplicate runs indicated that between 100–300 °C the maximum compressive strength was reached, which can be attributed to the promotion of polycondensation between chain-structures thus forming GP gels. In addition, between 300 °C to 700 °C, the residual compressive strength had deteriorated which can be assumed to occur owing to the thermal incompatibility between the paste and aggregate and also due to the fracture cracking brought about by the buildup of in situ pore pressures [22]. Sarker et al. [23] found that GP concrete cylinders have generally a higher conductivity than OPC concrete, owing in part to their relatively higher content of metal ions, such as, aluminum and iron. For these specimens, no spalling was found to occur and the ones with initial compressive strengths of 39–58 MPa had residual compressive strengths in the order of 83–59% at 650 °C, 27–29% at 800 °C and 16–18% at 1000 °C, respectively. The loss in strength was attributed to cracking and analysis by Scanning Electron Microscopy (SEM) confirmed that the GP matrix became denser at elevated temperatures, which might have provided the enhanced resistance to spalling.

Kong and Sanjayan [24] investigated the structural damage occurring to GP composites when exposed to elevated temperature. After exposure to 800 °C, GP paste gained 53% in strength, whilst the GP/aggregate composite had a strength reduction 63%. This is assumed to be due to the thermal incompatibility between GP binder and aggregate, which was subsequently proved by diametric measurements of GP and aggregate [25]. Kong et al. [26] concluded that the high permeability of the GP matrix allowed the moisture to escape, which in turn reduced the buildup of pore water pressures and the tendency of spalling to occur.

While GP concretes exhibit high resistance to elevated temperature levels, the high strengths achieved by RPCs cannot be generally matched. In addition to the relatively poor fire resistance of RPCs, they are also classified as materials that have a high carbon footprint, thus could result in additional adverse effects on the environment. In a study which tested the compressive strength of RPCs, where the binding material was replaced with FA and slag [27], a definite increase in the readings were reported in comparison to cement-based RPC, where all specimens achieved compressive strengths of over 200 MPa. In a similar study [28], the effects of using FA and slag as alternative materials for RPC production were investigated. At optimum proportions of the constituents of the mix design, the compressive strength reached up to 281 MPa. In a related study, it was also revealed that a combined RPC and GP concrete will contribute considerably to sustainable development, while lowering environmental impact and concomitantly providing efficient structural performance [29]. Obviously, a thorough comparative study of these two materials, especially at elevated temperature levels is highly desirable.

Despite several studies were conducted on GP and RPC, research regarding the behaviour of a combination of RPC and GP under fire-related scenarios is rather limited. Therefore, the novelty of the current work directly stems from the fact that it encompasses an extensive experimental program on Fly Ash (FA)-based GP pastes, RPC and a combined FA-based RPC and activated using sodium-based alkaline solutions—called Reactive Powder Geopolymer Concrete (RPGC). Factors such as characteristic strength, workability, conditioning parameters, production methods along with the residual strength, thermal cracking and weight loss parameters at elevated temperatures were investigated, through a series of controlled laboratory tests.

2. Materials and Methods

This section describes the experimental procedures carried out for the current study, including, materials, sample preparation, mixing and conditioning and testing of cubical samples. Parameters such a density, workability, compressive strength before and after exposure to elevated temperatures and weight losses were also measured. All the tests were conducted under laboratory conditions. Here we have also observed that the results obtained, typically over triplicate measurements, were reasonably precise. Hence the averages are quoted in the respective tables and the standard deviations are shown in the graphical representations.

2.1. Materials

2.1.1. Geopolymer (GP)-Based Pastes

The fly ash (FA) utilized in this investigation was obtained from Gladstone power station in Queensland, Australia (Class F- low calcium FA: ASTM C618 [30]. The chemical composition, obtained X-Ray Fluorescence (XRF) analysis and as reported by the manufacturer, is shown in Table 1. The various physical properties of FA, such as, particle size distribution, mean particle diameter, specific surface area, average pore diameter and pore volume are also given.

The information regarding the particle size distribution and average diameter were also available from the supplier—these parameters were measured by using a CILAS Particle Size Analyzer 1190. The particle shape analyses were performed by using a Zeiss Supra 40 VP Scanning Electron Microscope (SEM); however, the actual SEM images were not made available owing to commercial sensitivity. The samples were thinly gold coated with a DYNAVAC (CS 300) deposition system prior to the SEM analysis. The specific surface area and pore properties of FA were based on the nitrogen adsorption method, by using Belsorp Max equipment (i.e., by using Brunauer–Emmett–Teller (BET) theory-BELMasterTM Version 6.3.1.0 software, which was developed by BEL Japan, Inc., Osaka, Japan) [31]. Here, the amount of adsorbed gas to a monomolecular layer on the surface corresponds to a specific surface area and pore volume value.

Table 1. Chemical compositions of FA.

Compound	Oxide (wt. %)
SiO_2	51.1
Al_2O_3	25.6
Fe_2O_3	12.5
CaO	4.30
K_2O	0.70
MgO	1.45
Na_2O	0.77
TiO_2	1.32
BaO	0.09
SO_3	0.24
P_2O_5	0.89
MnO	0.15
Volatile fraction	0.89

Figure 1 shows the particle size distribution for the Gladstone based fly ash. The density of the sample was determined to be 2.29 g/cm^3. The largest particle diameter measured for Gladstone fly ash was 100 μm, with 50% of Gladstone fly ash particle size ranging from 1 μm to 100 μm and 50% are under 1 μm in size. The pore volume was determined to be 3.39 mm^3/g and the mean pore diameter was 11.8 nm. The specific surface area of the Gladstone fly ash was 1.15 m^2/g which was in agreement with previously reported results [32].
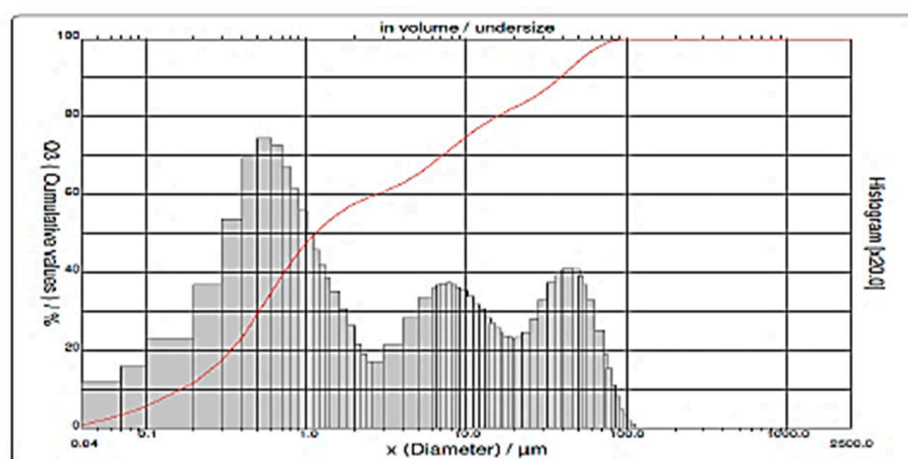
Figure 1. The aggregate particle size distribution graph for Gladstone FA.

The alkaline activator that was employed constituted of Grade D sodium silicate (ratio of SiO_2 to Na_2O is 1:2 by weight) and 8.0 M sodium hydroxide, NaOH. The sodium hydroxide solution consisted of 26.2 wt. % of NaOH solids and 73.8 wt. % of water [33]. A total of 10 alkaline activator combinations were investigated in this study and they consisted of varying the ratio of Na_2SiO_3/NaOH, from 0.5, 1.0, 1.5, 2.0 and 2.5 and at two alkaline solution to FA ratios of 0.4 and 0.57. These combinations are referred in the text as GP 01, GP 02 etc., as summarized in Table 2, which also presents the complete mix design proportions in each case.

Sodium hydroxide and sodium silicate were first measured and mixed using a hand-held stirrer bar until a clear, transparent solution was formed (ca. 2 min). The mixture was then kept aside to rest for 3 min before being mixed with the FA. This method was essentially adopted from a previously published work by Hardjito and Rangan [34]. Subsequently, the FA was measured and mixed with the liquid solution, using a *Breville* mixer at a working speed of 50 revolutions per minute (rpm) for 2 min and then for another 3 min at a working speed of 85 rpm, after which, 25 mm^3 specimens were casted.

Table 2. GP paste mix design.

Sample ID	Sample Composition for 1 kg of FA- (Alkaline Solution/FA Ratio; Na_2SiO_3/NaOH)	Sodium Silicate Grade D (kg)	8 M NaOH (kg)	Total Weight (kg)
GP 01	GP-0.40; 0.50	0.133	0.267	1.40
GP 02	GP-0.40; 1.00	0.200	0.200	1.40
GP 03	GP-0.40; 1.75	0.255	0.145	1.40
GP 04	GP-0.40; 2.00	0.267	0.133	1.40
GP 05	GP-0.40; 2.50	0.286	0.114	1.40
GP 06	GP-0.57; 0.50	0.190	0.380	1.57
GP 07	GP-0.57; 1.00	0.285	0.285	1.57
GP 08	GP-0.57; 1.75	0.363	0.207	1.57
GP 09	GP-0.57; 2.00	0.380	0.190	1.57
GP 10	GP-0.57; 2.50	0.407	0.163	1.57

The cubical samples were sealed immediately after casting in oven bags to minimize the effects of initial surface evaporation. The sealed specimens were subjected to oven conditioning, at 60 °C for 24 h in a *WEISS WVC Series Temperature and Climatic Test Chamber*. Once hardened, the cubes were removed from the molds, re-sealed and placed in the oven. The initial compressive strengths were tested after 24 h of curing and residual strengths were tested after exposure to 400 °C and 800 °C using the process defined in Section 3.2.

2.1.2. Reactive Powder-Based Concrete (RPC)

Type 1 Bastion General Purpose cement, supplied by DINGO Cement Pty Ltd., Burwood, Australia, complying with *AS 3972–2010-General purpose and blended cements* [35] and silica fumes, supplied from Master Builders Solutions by BASF, Australia, were used as the binder materials. The silica fumes were grey in color, comprised of very fine, spherical particles and met the requirements of *AS/NZS 3582.3:2016–Supplementary cementitious materials. Part 3–Amorphous silica* [36]. An XRF analyzer was used to determine the chemical compositions of silica fumes and the relevant data were supplied by the manufacturer (Table 3). Processed 50 N silica sand, with a maximum particle size of 600 μm, obtained from North Stradbroke Island, Australia and silica flour, which was white in color and supplied from Unimin Australia Ltd., Nyora, Australia, were used as the aggregate particles.

Table 3. Chemical composition of silica fumes.

Compound	Component (wt. %)
Al_2O_3	0.70
SiO_2	95.5
CaO	0.40
Fe_2O_3	0.30
K_2O	1.00
MgO	0.50
Na_2O	0.40
Other	1.20

With regard to the liquid components used in the RPC mixtures, *Glenium 51* high range water reducer was the superplasticiser (SP) used which was based on the work reported by Menefy [6], along with normal tap water. Three RPC mix designs were initially selected according to literature precedents (see in Table 4). However, the initial mixing processes resulted in poor workability—hence, mix design combinations were refined (Table 4). An excess amount of water was added to the aggregate particles in order to achieve saturated surface dry (SSD) conditions.

Table 4. Mix combinations of RPC, including refined combinations.

Sample ID	RPC 01-a	RPC 01-b	RPC 02	RPC 03
Amount needed (m^3)	1.0	1.0	1.0	1.0
Total weight initial (kg)	2212	2212	2398	2249
Cement (kg)	680	680	955	830
Silica fumes (kg)	204	204	229	291
Silica flour (kg)	204	204	10.0	488
Silica sand (kg)	974.0	974.0	1051	489.0
SP (mL)	44,000	44,000	13,000	55,000
Water (kg)	150	150	153	151
Initial w/c	0.22	0.22	0.16	0.18
Absorption by total sand %	1.0	1.0	1.0	1.0
Added water for absorption (kg)	11.7	11.7	10.6	10.6
Added superplasticiser (mL)	0.0	2.0	16	0.0
Added water (kg)	0.0	0.0	0.0	0.0
Final w/c	0.22	0.22	0.16	0.18
Super of cement + cume %	4.9	4.9	1.0	4.9
Final weight (kg)	2224	2224	2409	2259
Original reference	[37]	[37]	[2]	[27]

Mixing times and the rate of mixing were reported to be the crucial parameters, especially, in achieving high performances. Several reports have described the mixing processes, where the dry materials that are needed to be initially machine mixed for a period of 3–5 min at low speeds, after which the liquids are required to be added and then machine mixed for about 5–10 min. However, these time periods are known to vary among the various studies [27,38–42]. In addition, high energy machine mixers at shorter mixing times are proved to provide workable mixtures [6,43].

In the present study, the mixing procedure of RPC formulations were very similar to the one reported by Menefy [6], who has also referred to a typical staged- mixing approach as previously published [44]. Here, the dry materials (cement, silica fumes, silica sand and silica flour) were measured and machine-blended using a *Breville* mixer for 2 min at a working speed of 50 rpm until the dry materials reached homogeneous consistency. Subsequently, the super plasticizer (SP) and water were pre-mixed and added into dry mix. This was then machine-mixed for 30 min at 85 rpm until a workable mixture was obtained. A delayed addition of superplasticizer was effected for RPC 01-a and RPC 02 mixtures with a view to obtaining a SP to cementitious material content of approximately 5 wt. %.

Subsequently, 25 mm^3 cubes were casted. After hardening, the RPC cubes were subjected to water curing at two different temperatures, 20 °C and at 75 °C, in a temperature-controlled water bath. This conditioning procedure was done in order to test the effects of ambient-temperature water-curing on the compressive strength of the samples that were conditioned for 7 days. Such samples were labelled RPC 01-a.

2.1.3. Reactive Powder Geopolymer Concrete (RPGC)

The reactive powder geopolymer concrete (RPGC) was casted using a mix of GP and RPC. A total of four RPGC mixes were casted with zero utilization of cement. The starting ingredients, such as, solid materials (FA, silica fumes, silica sand and silica flour) and liquid components (alkaline solution, SP and water) used to cast RPGC specimens, were the same as those used to cast GP pastes and RPC test samples. The corresponding mix design specifications are given in Table 5.

During mixing of RPCG, dry materials were machine mixed using a *Breville* mixer until homogeneity was reached (ca. 2 min at 50 rpm). The liquid solution (sodium hydroxide, sodium silicate and water) were premixed for 1 min and added with the dry ingredients. The resulting formulation was machine mixed for a further 2 min at 50 rpm and then for 3 min at 85 rpm.

Table 5. Mix Design—RPGC Trial and Error.

Mix Components Sample ID	RPC01 + Gladstone GP-0.4/2.5 RPGC 01	RPC02 + Gladstone GP-0.4/2.5 RPGC 02	RPC01 + Gladstone GP-0.57/2.5 RPGC 03	RPC02 + Gladstone GP-0.57/2.5 RPGC 04
Volume needed (mm^3)	1.00	1.00	1.00	1.00
GP cement (kg/m^3)	—	—	—	—
Fly ash (kg)	680	955	680	955
Silica fume (kg/m^3)	204	229	204	229
Silica flour 200 G (kg/m^3)	204	10.0	204	10.0
Silica sand 50 N (kg/m^3)	974	1051	974	1051
Alkaline solution (kg)	272	382	388	544
8 M NaOH (kg)	77.7	109	111	156
Sodium silicate grade D (kg)	194	273	277	389
SP (L/m^3)	—	—	—	—
Water (kg/m^3)	—	—	—	—
Added water due to absorption (kg)	11.7	10.6	11.7	10.6
Added water due to workability (kg)	—	—	—	—
Alkaline solution/fly ash ratio	0.40	0.40	0.57	0.57
Na_2SiO_3/NaOH	2.50	2.50	2.50	2.50
Aggregate/binder ratio	2.03	1.35	2.03	1.35
Total weight (kg)	2334	2627	2450	2789

Following on from above, 25 mm^3 RPGC specimens were casted. The curing conditioning procedure for RPGC was similar to GP paste specimens, where sealed cubes were subjected to dry oven curing at 60 °C for 24 h in a *WEISS WVC Series Temperature and Climatic Test Chamber*. Subsequently, initial strength and residual strength testing was conducted.

2.2. Exposure to Elevated Temperatures (Up to 400, or 800 °C)

All samples were subjected to the same levels of exposure to the elevated temperatures (up to 400, or 800 °C, as the case may be). During the exposure, heating was provided at a steady rate of 10 °C/min, up to the target temperatures, using a muffle furnace. The samples were held at the target temperature for a period of one hour, in order to ensure that the entire sample has obtained thermal equilibrium, i.e., a uniform temperature throughout the sample. The samples were then allowed to cool naturally to room temperature (ca. 25 °C), before they were tested for compressive strength. It is to be noted here that testing of specimens for residual compressive strength after they had been cooled down generally characterizes the lower bound strength values, as compared to the stressed residual test, where samples are tested whilst they are at elevated temperatures [45,46].

2.3. Testing Procedures

The density measurements on test samples were recorded in accordance with *AS 1012.5:2014—Determination of mass per unit volume of freshly mixed concrete* [47] and the workability was measured using a flow table apparatus, in accordance with *ASTM C230/230M-08—Standard Specification for Flow Table for Use in Tests of Hydraulic Cement* [48]. The compressive strength testing was conducted in accordance with *AS 1012.9.2014—Methods of testing concrete Method 9: Compressive strength tests—Concrete, mortar and grout specimens* [49] using a 100 kN *Instron* 1195 testing machine, at a loading rate of 20 ± 2 MPa/min. The cubical specimens were tested for initial compressive strength at 24 h after casting. No samples were subjected to a rest period, which meant that all samples were assumed to be immediately cured after casting. The measurements were done in triplicate and the average values are quoted. The mass loss for each test sample was measured using two methods: by using a balance and through thermo-gravimetric (TGA) runs. In the first method, cube samples were accurately weighed in an electronic balance before and after exposure to elevated temperature levels from which the difference in weights were calculated. In the

second method, the Mettler Toledo TGA was used to determine the loss of mass. Powdered samples (obtained passing through the 0.425 μm (ca. 20 mg) sieve were placed in silica crucibles and subjected to a constant heating rate of 10 °C/min up to 800 °C, under a nitrogen atmosphere and the mass loss of the samples (in wt. %) were recorded with increasing temperatures (from 30 to 800 °C).

3. Results and Discussion

It is relevant to note here that the various empirical parameters, such as density, workability, compressive strengths and mass losses, obtained were averaged over triplicate measurements as the spread of values were quite acceptable given the nature of specific measurements in question. Furthermore, the standard deviations in the case of residual strength recordings are shown in the corresponding plots.

3.1. Slump Flow Characteristics of the Mixtures

The workability of fresh admixtures is an important factor to assess and evaluate the overall performance of concretes. Any given mix design is expected to maintain its fluid nature to enable mixing, transportation, placement and finishing procedures. The GP pastes in present study exhibited excellent workability parameters, which was expected as the mix matrix comprised of very fine and spherical shaped particles which are bestowed with a smooth flow character. The slump flow of GP 01–05 was lower than for GP 06–10, except for GP 07; this can be attributed to the higher alkaline solution to FA ratio of the latter half of the mixtures. The higher this ratio implies a higher fluid content in the mixture which produce a more liquid paste (see the results given in Table 6).

Table 6. Workability results for GP paste mixtures.

Sample ID	d1 (mm)	d2 (mm)	Slump Flow (mm)
GP 01	300	300	300.0
GP 02	300	305	302.5
GP 03	315	310	312.5
GP 04	300	300	300.0
GP 05	290	300	295.0
GP 06	305	310	307.5
GP 07	280	280	280.0
GP 08	310	320	315.0
GP 09	330	340	335.0
GP 10	320	330	325.0
Minimum	280	280	280.0
Maximum	330	340	335.0

The Slump Flow results for RPC mixes are given in Table 7. Compared to the GP mixtures, RPC specimens displayed relatively low workability attributes, with a minimum slump flow of 111.0 mm and maximum of 132.5 mm. This condition can be expected owing to the inclusion of aggregate particles which can increase the friction among the constituents and hence result in a decreased flow characteristics. Moreover, the RPC mixtures were observed to be denser compared to the GP pastes, which further reduces the workability characteristics of the mixture. The Flow Table results obtained in this study were found to be lower than the ASTM C230 standard requirement, which is 190 mm–250 mm after 20 drops. According to Gowripalan and Watters [37], this flow can be achieved with a mixing time of about 40 min at laboratory conditions.

The RPGC mixtures recorded a higher slump flow compared to RPC mixes, which could be due to the finer and spherical nature of the FA and this in turn can be assumed to improve the fluidity and workability conditions of the former. In contrast, RPGC formulations were appeared to be more viscous compared to GP paste mixes, thus recording poorer flow readings which could be due to the inclusion on aggregate particles which effectively could thicken the mixture, thus reducing the workability conditions. In addition,

it can be noted that the flow-ability of RPGC 01 and 02 are much lower than RPGC 03 and 04. This can be attributed to the value of the alkaline solution to FA ratio of the latter two mixtures (0.57), as compared to the former two mixtures (0.4), thus producing a more workable mix. The slump flow results are given in Table 8.

Table 7. Workability results RPC mixtures.

Sample ID	d1 (mm)	d2 (mm)	Slump Flow (mm)
RPC 01-a	130	135	132.5
RPC 01-b	120	120	120.0
RPC 02	110	112	111.0
Minimum	110	112	111.0
Maximum	130	135	132.5

Table 8. Workability results RPGC mixtures.

Sample ID	d1 (mm)	d2 (mm)	Slump Flow (mm)
RPGC 01	190	185	187.5
RPGC 02	223	225	224.0
RPGC 03	254	250	252.0
RPGC 04	250	250	250.0
Minimum	190	185	187.5
Maximum	254	250	252.0

3.2. Density Measurements

The values of density of the RPC mixtures were much higher than that of both GP and RPGC mixtures, with the highest reading of 2752 kg/m^3 recorded for RPC 01-b (Table 9). This can be expected as RPC is an ultra-high strength concrete, having very fine particles which provide a highly dense microstructure. The densest GP paste mix turned out to be GP 10, with a density of 2396 kg/m^3 (Table 10). The RPGC mixtures, on the other hand, displayed a maximum density of 2245 kg/m^3 (for RPGC 01) and a minimum of 2120 kg/m^3 (for RPGC 04) (Table 11).

Table 9. Density results of RPC mixtures.

Sample ID	Mass (kg)	Density (kg/m^3)
RPC 01-a	0.2546	2546
RPC 01-b	0.2752	2752
RPC 02	0.2715	2715

Table 10. Density results of GP paste mixtures.

Sample ID	Mass (kg)	Density (kg/m^3)
GP 01	0.2189	2189
GP 02	0.2272	2272
GP 03	0.2154	2154
GP 04	0.2335	2335
GP 05	0.2364	2364
GP 06	0.2203	2203
GP 07	0.2298	2298
GP 08	0.2308	2308
GP 09	0.2371	2371
GP 10	0.2396	2396

Table 11. Density results of RPGC mixtures.

Sample ID	Mass (kg)	Density (kg/m^3)
RPCG 01	0.2245	2245
RPCG 02	0.2193	2193
RPCG 03	0.2145	2145
RPCG 04	0.2120	2120

3.3. Evaluations of Initial and Residual Strengths

When considering the initial compressive strengths of GP specimens, majority of specimens having a lower alkaline solution to FA ratio (0.4) achieved higher initial strengths, when the Na_2SiO_3/NaOH ratios were kept constant. This could probably be due to the dense microstructure brought about from using a lower alkaline solution to FA ratio, which could result in fewer pores and hence higher internal strengths. In addition, when the alkaline solution to FA ratio was kept constant, the initial strength of the specimens were found to increase gradually as the Na_2SiO_3/NaOH ratios increased, which could be attributed to the inclusion of more sodium silicate, which in turn can enhance the geopolymerization reaction, thus resulting in higher strengths (Figure 2).
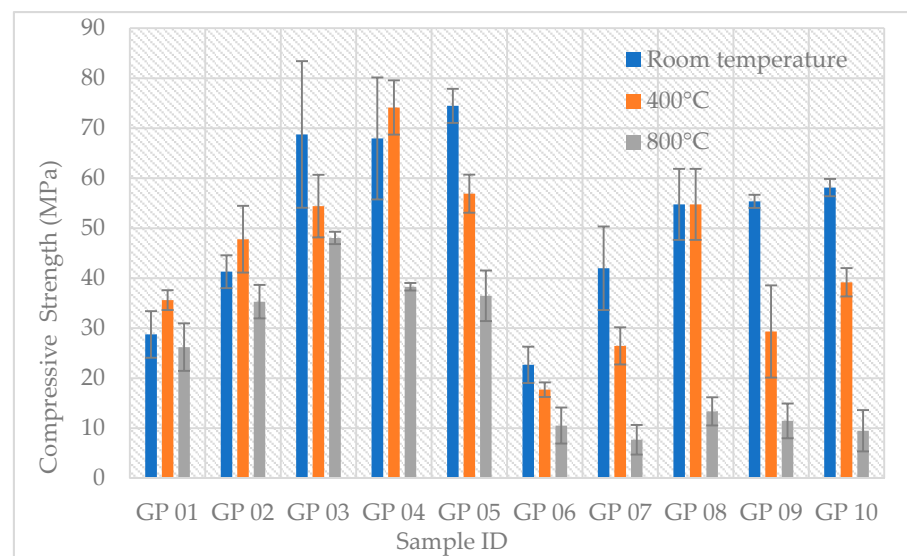
Figure 2. A plot of initial and residual compressive strengths of GP specimens.

After exposure to elevated temperature levels of 800 °C, majority of the GP specimens were found to be still intact with only mild cracking. Furthermore, no cracking was observed in GP 01–05 specimens after being exposed to both 400 °C and 800 °C and mild cracking in the latter set of samples (i.e., GP 06–10), that too only after being exposed to 800 °C. Owing to the high initial strengths and thermal performance of GP 05 and GP 10, they were explored for further mix designs leading to the production of RPGC specimens.

When considering the initial strength developments of RPC specimens, conditioning was found to be a highly influential factor, where specimens conditioned at 25 °C recorded much lower 7-day-strength readings compared to the specimens cast using the same mix design, but conditioned at 75 °C. The tabulated and associated graphical representation of, data are presented in Table 12 and Figure 3, respectively. Similar finding were reported previously [6,50], where it was also stated that a relatively lower percentage of calcium-silicate-hydrate (C-S-H) gels were produced, when an insufficient supply of heated water was provided, which was assumed to create a weaker microstructural matrix within RPC specimens. A previous report also showed that when RPC was water cured under room temperature, the pozzolanic activity was found to be slower, as heated water curing has the ability to rapidly increase the pozzolonic reaction of the silica fumes and increase the

amounts of hydrated compounds occurring through the formation of secondary hydrated products. This, in turn can result in an increased extent of bonding between the cement paste and the aggregate particles, thus enhancing the internal strength. In addition, the formation of ettringite can hinder the rate of hydration thus, reduces the rate of strength development [42]. Moreover, a continuous supply of moisture can result in a higher consumption of portlandites, which can further lead to a higher degree of hydrated products. These hydrated products could act as an inert filler material which could in turn fill the voids and gel pores within the matrix. This could ultimately a lead to denser microstructure with a better interlocking structure and fewer capillary pores- similar findings were reported previously [6,42,51].

Table 12. Average compressive strengths of RPC cubes.

| Sample ID	Average Initial Compressive Strength (MPa)
RPC 01-a (25 °C)	86.0
RPC 01-a (75 °C)	141
RPC 01-b (75 °C)	95.1
RPC 02 (75 °C)	108
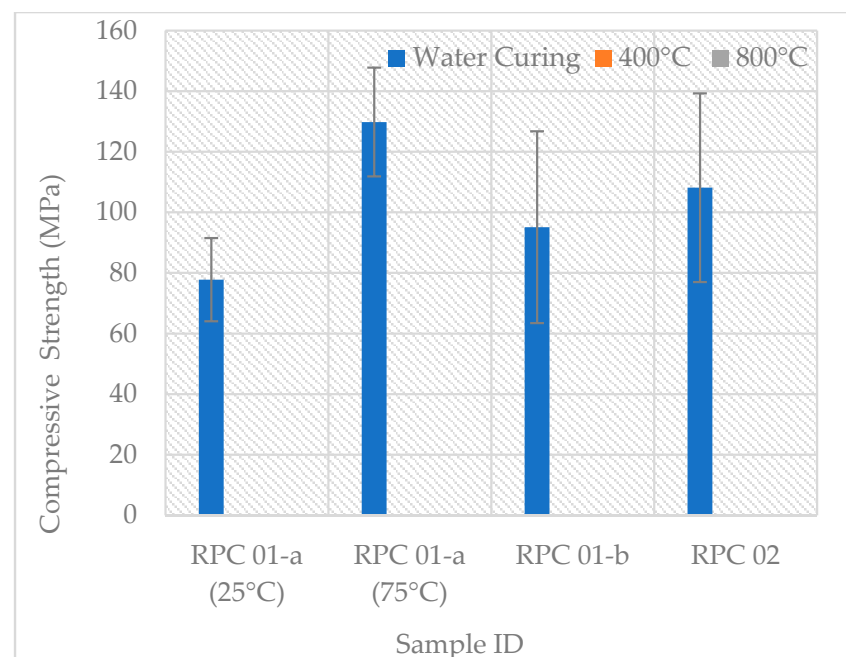
Figure 3. A plot of average initial compressive strengths of RPC specimens.

Regardless of the very high initial performances, the RPC specimens exhibited completely different thermal performances. These samples displayed explosive spalling phenomenon when the furnace temperature reached approximately 360 °C; hence no residual strength results could be measured. The occurrence of explosive spalling in the present study can be attributed to the formation of dense microstructures which in turn could limit the release of the internal pressure build-up during heating. Concomitantly, the occurrence of thermal gradients between the outside and the inside of the concrete could give rise to associated thermal stresses and once these stresses exceed the tensile strength, spalling can be expected to occur. Similar reports on the poor thermal capabilities of RPC have been presented elsewhere [52–54]. Figure 4 shows the RPC specimens before and after exposure to elevated temperatures.

Figure 4. RPC specimens before (**left**) and after (**right**) exposure to elevated temperatures.

The RPGC 01 specimens, which was a combination of GP 05 and RPC 01-a, performed the best in terms of initial compressive and residual strengths, with an initial strength of approximately 76 MPa and residual strengths of approximately 61 MPa and 51 MPa at 400 °C and 800 °C, respectively (Table 13). It was also noted that at a lower alkaline solution to FA ratio and a high silica flour content, improved strengths, both initial and residual, can be achieved. Thus the low alkaline solution to FA ratio could provide a denser microstructure with reduced porosity and hence can increase the bondage between the paste and the aggregate particles. The high flour content can be advantageous as the silica content can increase the pozzolanic reaction and can also act as a filler which can further increase internal strength. Similar observations were previously reported [55].

Table 13. Average compressive strengths of RPGC cubes.

Sample ID	Room Temperature	400 °C	800 °C	Thermal Cracking 400 °C	Thermal Cracking 800 °C
RPCG 01	76.25	60.58	50.52	No	No
RPCG 02	64.54	44.43	30.58	No	No
RPCG 03	38.59	21.67	14.90	No	Yes
RPCG 04	19.55	18.34	14.42	No	No
Minimum	19.55	18.34	14.42	N/A	N/A
Maximum	76.25	60.58	50.52	N/A	N/A

The RPGC specimens were observed to behave exceptionally well after exposure to a high temperature; for instance, no cracking was evident from any of the specimens after exposure to 400 °C. Additionally, apart from RPGC 03 specimens which displayed slight cracking, no other specimens displayed any cracking even after being exposed to 800 °C. The RPGC specimens produced strengths within the range of approximately 18–61 MPa at 400 °C and approximately 14–51 MPa at 800 °C, with maximum strength drops of approximately 20% and 33% at 400 °C and 800 °C, respectively. In particular, RPGC 04 proved to be the weakest mixture producing the lowest initial and residual strength readings. Figure 5 shows a graphical representation of the strengths of RPGC specimens.

3.4. Mass Loss Measurements

Table 14 shows the percentage mass loss values from TGA (powdered samples) and 25 mm cubes measured by using a balance for GP paste specimens. The average values of the mass loss measurements using the balance were approximately 17% for samples after being exposed to temperatures of both 400 °C and 800 °C. The specimens that were subjected to the thermo-gravimetric analysis (TGA showed relatively much lesser losses, with averages of approximately 7.5% and 9.4% for 400 °C and 800 °C exposure, respectively. This difference in mass loss percentages could be due to the severe thermal cracking, which could have caused minor corner spalling to occur in the cube specimens, thus resulting in

higher losses. However, it may be noted here that mass measurements taken on bulk samples (i.e., cubes) can be considered to be more reliable than the corresponding ones obtained through TGA runs as inhomogeneity of the samples can be considered to be amplified in mg scales (i.e., in the case of thermograms obtained from the TGA runs). When considering the high initial rate of mass loss can be attributed to the evaporation of physically bound (free) moisture, after which the rate reduces and somewhat stabilizes [25,56–59]. The continued loss in mass after the initial steep drop, can be due to the loss of chemically bound water and in part resulting from the decomposition of $CaCO_3$ (ca. 700 to 800 °C) within the concrete matrix [57].
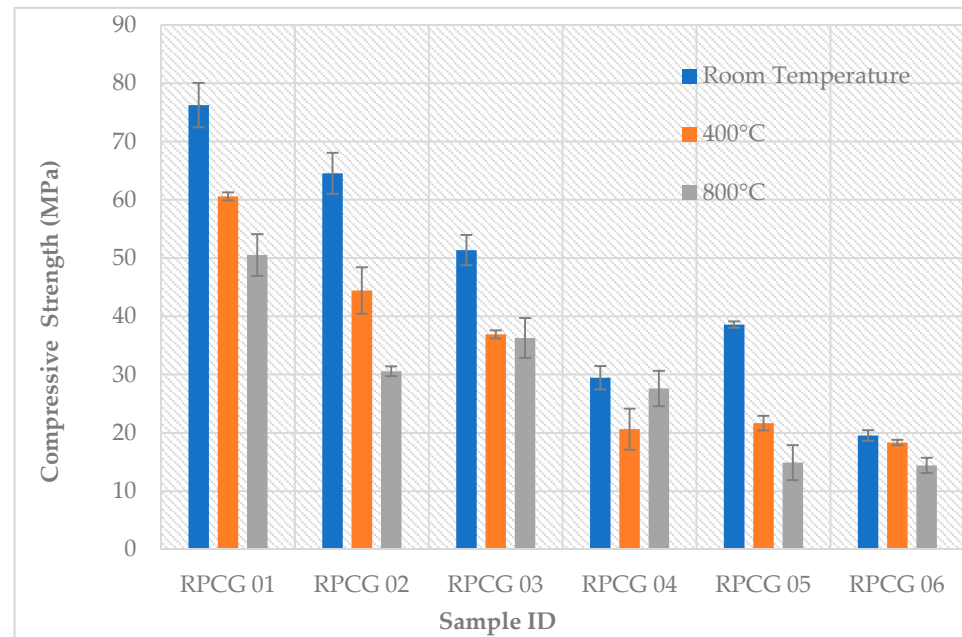

Figure 5. A plot of average initial and residual compressive strengths of RPGC specimens.

Table 14. Average compressive strengths of RPGC cubes.

Sample ID	Mass Loss (wt. %) from TGA		Mass Loss (wt. %) from Weighing	
	400 °C	800 °C	400 °C	800 °C
GP 01	6.47	8.45	14.10	15.88
GP 02	6.59	8.09	14.61	15.34
GP 03	7.16	8.73	14.08	14.86
GP 04	6.66	7.78	15.09	15.37
GP 05	6.73	7.84	15.08	15.79
GP 06	7.89	10.56	22.39	21.68
GP 07	8.66	11.76	20.33	20.99
GP 08	8.36	10.69	19.27	19.52
GP 09	8.64	10.22	19.66	19.31
GP 10	7.89	9.65	19.75	20.04
Minimum	6.47	7.78	14.08	14.86
Maximum	8.66	11.76	22.39	21.68
Average	7.51	9.38	17.43	17.88

The RPGC specimens recorded the lowest percentages in mass losses, from TGA runs and measurements using a balance, as compared to the GP paste specimens. This could be due to the higher percentage of solid particles (and hence lower water loadings) within the RPGC specimens as compared to the GP specimens. Hence, the overall loss of mass is potentially reduced as mass loss can be thought to arise mainly from the loss of moisture. In addition, among the RPGC specimens, RPGC 01 cube specimens recorded to be the densest (i.e., having a density value of 2245 kg/m^3). This effectively means that a lower

percentage of moisture was available for evaporation at elevated temperature levels; hence, would result in lower mass losses. Similar assumptions were made in previous studies involving the testing of conventional and GP concretes [23,60]. Additionally, compared to OPC concretes which continue to have a consistent rate of mass loss up to 650 °C due to the dehydration of $Ca(OH)_2$, the RPGC specimens recorded a reduced rate of mass loss above a temperature of 400 °C, which indicate that the RPGC specimens have a relatively higher storage capacity and thermal stability- these features could also help them maintain their structural integrity even at higher temperatures. Table 15 provides tabulated data of the percentage mass losses of the RPGC specimens.

Table 15. Percentage mass loss (TGA and Balance results)–RPGC.

Sample ID	Mass Loss (wt. %) from TGA		Mass Loss (wt. %) from Weighing	
	400 °C	800 °C	400 °C	800 °C
RPGC 01	3.06	3.97	6.750	5.600
RPGC 02	3.75	4.81	8.060	8.070
RPGC 03	5.00	5.86	9.000	9.030
RPGC 04	5.95	6.64	11.23	11.32
Minimum	3.06	3.97	6.750	5.600
Maximum	5.95	6.64	11.23	11.32
Average	4.44	5.32	8.760	8.510

In summary, the RPGC specimens tested after a conditioning period of 24 h at 60 °C displayed higher strength readings, with a highest initial strength value of approximately 76 MPa for RPGC 01. This is somewhat similar to the initial strength reading recorded from GP 05 with an increase of about 2 MPa, with RPGC 01 being the higher of the two. In addition, RPGC 01 recorded the highest residual strength after being exposed to 800 °C compared to all the GP specimens.

4. Conclusions

This research was focused on investigating the performance of a novel material called reactive powder geopolymer concrete (RPGC). Class-F (low calcium) FA was used as the source material, which effectively eliminated the need to use ordinary Portland cement in the mix design. The RPGC formulations were a combination of the geopolymer (GP) paste and reactive powder concrete (RPC) mix designs, selected through a series of trial tests. Even though several studies have been reported on the performance of GPs and RPCs, the available literature on the mechanical properties and, most importantly, the fire performance of the combination of these two materials are scarce. The key finding from the present study can be summarized as follows:

- Generally, the RPC samples that were investigated in the present study produced low workability conditions as compared to the GP and RPGC samples.
- The RPGC specimens, on the other hand, displayed higher workability conditions. This can be due to the relatively smaller particle sizes of the FA used for the casting of RPGC samples, as compared to the cement in RPC ones.
- The slump flow values of the RPGC specimens were somewhat lower when compared to the corresponding values of the GP mixtures. This can be attributed to the inclusion of aggregate particles in the RPGC formulations. The RPC specimens that were conditioned at 75 °C recorded higher compressive strengths compared to those conditioned at the ambient temperature. This can be assumed to arise from the formation of relatively denser microstructures, thus leading to a better cohesive bonding state.
- Furthermore, the RPC specimens were found to undergo explosive spalling, at an elevated temperature (ca. 360 °C), presumably owing to the built up of increased vapor pressure and higher thermal gradients.
- Unlike the RPC specimens, no explosive spalling conditions were apparent in the RPGC specimens, with no thermal cracking at 400 °C and only one of the specimens

undergoing mild thermal cracking even at 800 °C. This can be due to the higher levels of silicon in the FA compared to OPC.

- The RPGC specimens generally recorded lower percentage losses in mass compared to the GP specimens, which could be due to the reduced water loading in them.

References

1. Team, E. *Reactive Powder Concrete*; Purdue ECT Team, Purdue University: West Lafayette, Indiana, 2007.
2. Richard, P.; Cheyrezy, M.H. Reactive Powder Concretes with High Ductility and 200–800 MPa Compressive Strength. *Spec. Publ.* **1994**, *144*, 507–518.
3. Richard, P.; Cheyrezy, M. Composition of Reactive Powder Concretes. *Cem. Concr. Res.* **1995**, *25*, 1501–1511. [CrossRef]
4. Lee, M.-G.; Wang, Y.-C.; Chiu, C.-T. A Preliminary Study of Reactive Powder Concrete as a New Repair Material. *Constr. Build. Mater.* **2007**, *21*, 182–189. [CrossRef]
5. Chan, Y.-W.; Chu, S.-H. Effect of Silica Fume on Steel Fiber Bond Characteristics in Reactive Powder Concrete. *Cem. Concr. Res.* **2004**, *34*, 1167–1172. [CrossRef]
6. Menefy, L. *Investigation of Reactive Powder Concrete and It's Damping Characteristics When Utilised in Beam Elements*; Griffith University: Gold Coast, QLD, Australia, 2007.
7. Coppola, L.; Troli, R.; Borsoi, A.; Zaffaroni, P.; Collepardi, M. Influence of Superplasticizer Type on the Compressive Strength of RPM. In *Proceedings of the Fifth CANMET/ACI International Conference on Superplasticizers and Other Chemical Admixtures in Concrete, Roma, Italy*; ACI International: Farmington Hills, MI, USA, 1997.
8. Peng, G.-F.; Kang, Y.R.; Huang, Y.Z.; Liu, X.P.; Chen, Q. Experimental Research on Fire Resistance of Reactive Powder Concrete. *Adv. Mater. Sci. Eng.* **2012**, *2012*, 860303. [CrossRef]
9. Tian, K.P.; Ju, Y.; Liu, H.B.; Liu, J.H.; Wang, L.; Liu, P.; Zhao, X. Effects of Silica Fume Addition on the Spalling Phenomena of Reactive Powder Concrete. In Applied Mechanics and Materials. *Trans. Tech. Publ.* **2012**, *174*, 1090–1095.
10. So, H.-S.; Yi, J.B.; Khulgadai, J.; So, S.Y. Properties of Strength and Pore Structure of Reactive Powder Concrete Exposed to High Temperature. *ACI Mater. J.* **2014**, *111*, 335–346. [CrossRef]
11. Zheng, W.; Luo, B.; Wang, Y. Compressive and Tensile Properties of Reactive Powder Concrete with Steel Fibres at Elevated Temperatures. *Constr. Build. Mater.* **2013**, *41*, 844–851. [CrossRef]
12. Ju, Y.; Liu, H.; Tian, K.; Liu, J.; Wang, L.; Ge, Z. An Investigation on Micro Pore Structures and the Vapor Pressure Mechanism of Explosive Spalling of RPC Exposed to High Temperature. *Sci. China Technol. Sci.* **2013**, *56*, 458–470. [CrossRef]
13. Lloyd, N.; Rangan, V. Geopolymer Concrete with Fly Ash. In *Proceedings of the Second International Conference on Sustainable Construction Materials and Technologies*; UWM Center for By-Products Utilization: Milwaukee, WI, USA, 2010.
14. Davidovits, J. *Synthesis of New High-Temperature Geopolymers for Reinforced Plastics/Composites, in SPE PACTFC 79, Society of Plastic Engineers*; Brookfield Center: Fairfield County, CT, USA, 1979; pp. 151–154.
15. Davidovits, J. Geopolymers: Inorganic Polymeric New Materials. *J. Therm. Anal.* **1991**, *37*, 1633–1656. [CrossRef]
16. Lyon, R.E.; Balaguru, P.N.; Foden, A.; Sorathia, U.; Davidovits, J.; Davidovics, M. Fire-Resistant Aluminosilicate Composites. *Fire Mater.* **1997**, *21*, 67–73. [CrossRef]
17. Lee, W.K.W.; van Deventer, J.S.J. The Effect of Ionic Contaminants on the Early-Age Properties of Alkali-Activated Fly Ash-based Cements. *Cem. Concr. Res.* **2002**, *32*, 577–584. [CrossRef]
18. Wang, H.; Li, H.; Yan, F. Reduction in Wear of Metakaolinite-Based Geopolymer Composite through Filling of PTFE. *Wear* **2005**, *258*, 1562–1566. [CrossRef]

19. Palomo, A.; Blanco-Varela, M.T.; Granizo, M.L.; Puertas, F.; Vazquez, T.; Grutzeck, M.W. Chemical Stability of Cementitious Materials Based on Metakaolin. *Cem. Concr. Res.* **1999**, *29*, 997–1004. [CrossRef]
20. Duxson, P.; Lukey, G.C.; van Deventer, J.S.J. Thermal Conductivity of Metakaolin Geopolymers Used as a First Approximation for Determining Gel Interconnectivity. *Ind. Eng. Chem. Res.* **2006**, *45*, 7781–7788. [CrossRef]
21. Shaikh, F. Effects of Alkali Solutions on Corrosion Durability of Geopolymer Concrete. *Adv. Concr. Constr.* **2014**, *2*, 109–123. [CrossRef]
22. Türkmen, İ.; Karakoç, M.B.; Kantarcı, F.; Maraş, M.M.; Demirboğa, R. Fire Resistance of Geopolymer Concrete Produced from Elazığ Ferrochrome Slag. *Fire Mater.* **2016**, *40*, 836–847. [CrossRef]
23. Sarker, P.K.; Kelly, S.; Yao, Z. Effect of Fire Exposure on Cracking, Spalling and Residual Strength of Fly Ash Geopolymer Concrete. *Mater. Des.* **2014**, *63*, 584–592. [CrossRef]
24. Kong, D.L.; Sanjayan, J.G. Damage Behavior of Geopolymer Composites Exposed to Elevated Temperatures. *Cem. Concr. Compos.* **2008**, *30*, 986–991. [CrossRef]
25. Kong, D.L.Y.; Sanjayan, J.G. Effect of Elevated Temperatures on Geopolymer Paste, Mortar and Concrete. *Cem. Concr. Res.* **2010**, *40*, 334–339. [CrossRef]
26. Kong, D.; Sanjayan, J.; Sagoe-Crentsil, K. Comparative Performance of Geopolymers Made with Metakaolin and Fly Ash after Exposure to Elevated Temperatures. *Cem. Concr. Res.* **2007**, *37*, 1583–1589. [CrossRef]
27. Yazıcı, H.; Yardımcı, M.Y.; Aydın, S.; Karabulut, A.Ş. Mechanical Properties of Reactive Powder Concrete Containing Mineral Admixtures under Different Curing Regimes. *Constr. Build. Mater.* **2009**, *23*, 1223–1231. [CrossRef]
28. Yazıcı, H.; Yiğiter, H.; Karabulut, A.Ş.; Baradan, B. Utilization of Fly Ash and Ground Granulated Blast Furnace Slag as an Alternative Silica Source in Reactive Powder Concrete. *Fuel* **2008**, *87*, 2401–2407. [CrossRef]
29. Ng, T.S.; Voo, Y.L.; Foster, S.J. Sustainability with Ultra-High Performance and Geopolymer Concrete Construction. In *Innovative Materials and Techniques in Concrete Construction*; Springer: Dordrecht, The Netherlands, 2012; pp. 81–100.
30. ASTM C 618. *Standard Specification for Coal Fly Ash and Raw or Calcined Natural Pozzolan for Use in Concrete*; ASTM: West Conshohocke, PA, USA, 2012.
31. Brunauer, S.; Emmett, P.H.; Teller, E. Adsorption of Gases in Multimolecular Layers. *J. Am. Chem. Soc.* **1938**, *60*, 309–319. [CrossRef]
32. Pathan, S.M.; Aylmore, L.A.; Colmer, T.D. Properties of Several Fly Ash Materials in Relation to Use as Soil Amendments. *J. Environ. Qual.* **2003**, *32*, 687–693. [CrossRef]
33. Rangan, B.V. Fly Ash-Based Geopolymer Concrete. *Indian Concr. J.* **2006**, *80*, 35.
34. Hardjito, D.; Rangan, B.V. *Development and Properties of Low Calcium Based Geopolymer Concrete*; Curtin University of Technology: Perth, Australia, 2005.
35. Standard, A. *General Purpose and Blended Cements*; Standard Australian: Sydney, Australia, 2010.
36. Standard, A.N.Z. *Supplementary Cementitious Materials. Part 3: Amorphous Silica*; Standard Australian: Sydney, Australia, 2016.
37. Gowripalan, N.; Watters, R.; Gilbert, I.; Cavill, B. Reactive Powder Concrete (Ductal®) for Precast Structural Concrete–Research and Development in Australia. In Proceedings of the 21st Biennial Conference of the CIA, Brisbane, Australia, 18–21 July 2003.
38. Yazıcı, H.; Deniz, E.; Baradan, B. The Effect of Autoclave Pressure, Temperature and Duration Time on Mechanical Properties of Reactive Powder Concrete. *Constr. Build. Mater.* **2013**, *42*, 53–63. [CrossRef]
39. Zdeb, T. An Analysis of the Steam Curing and Autoclaving Process Parameters for Reactive Powder Concretes. *Constr. Build. Mater.* **2017**, *131*, 758–766. [CrossRef]
40. Mostofinejad, D.; Nikoo, M.R.; Hosseini, S.A. Determination of Optimized Mix Design and Curing Conditions of Reactive Powder Concrete (RPC). *Constr. Build. Mater.* **2016**, *123*, 754–767. [CrossRef]
41. Helmi, M.; Hall, M.R.; Stevens, L.A.; Rigby, S.P. Effects of High-Pressure/Temperature Curing on Reactive Powder Concrete Microstructure Formation. *Constr. Build. Mater.* **2016**, *105*, 554–562. [CrossRef]
42. Hiremath, P.N.; Yaragal, S.C. Effect of Different Curing Regimes and Durations on Early Strength Development of Reactive Powder Concrete. *Constr. Build. Mater.* **2017**, *154*, 72–87. [CrossRef]
43. Ma, J.; Orgass, M.; Dehn, F.; Schmidt, D.; Tue, N.V. Comparative Investigations on Ultra-High Performance Concrete with and without Coarse Aggregates. In Proceedings of the International Symposium on Ultra High Performance Concrete, Kassel, Germany, 13–15 September 2004.
44. Bonneau, O.; Lachemi, M.; Dallaire, E.; Dugat, J.; Aitcin, P.C. Mechanical Properties and Durability of Two Industrial Reactive Powder Concretes. *Mater. J.* **1997**, *94*, 286–290.
45. Phan, L. *Fire Performance of High-Strength Concrete: A Report of the State of-the-Art*; Building and Fire Research Laboratory, National Institute of Standards and Technology: Gaithersburg, MD, USA, 1996.
46. Guerrieri, M.; Sanjayan, J.G. Behavior of Combined Fly Ash/Slag-Based Geopolymers When Exposed to High Temperatures. *Fire Mater.* **2010**, *34*, 163–175. [CrossRef]
47. Standard, A. *Methods of Testing Concrete Method 5: Determination of Mass Per Unit Volume of Freshly Mixed Concrete*; Standard Australian: Sydney, Australia, 2014.
48. ASTM C230/C 230M–03. *Standard Specification for Flow Table for Use in Tests of Hydraulic Cement*; ASTM: West Conshohocken, PA, USA, 2008.

49. Standard, A. *Methods of Testing Concrete. Method 9: Compressive Strength Tests—Concrete, Mortar and Grout Specimens*; Standards Australia Limited: Sydney, Australia, 2014.
50. Khadiranaikar, R.; Muranal, S. Factors Affecting the Strength of Reactive Powder Concrete (RPC). *Int. J. Civil. Engg. Tech.* **2012**, *3*, 455–464.
51. Courtial, M.; de Noirfontaine, M.N.; Dunstetter, F.; Signes-Frehel, M.; Mounanga, P.; Cherkaoui, K.; Khelidj, A. Effect of Polycarboxylate and Crushed Quartz in UHPC: Microstructural Investigation. *Constr. Build. Mater.* **2013**, *44*, 699–705. [CrossRef]
52. Liu, H.; Li, K.L.; Ju, Y.; Wang, H.J.; Wang, J.B.; Tian, K.P.; Wei, S. Explosive Spalling of Steel Fiber Reinforced Reactive Powder Concrete Subject to High Temperature. *Concrete* **2010**, *8*, 6–8.
53. Ju, Y.; Liu, J.; Liu, H.; Tian, K.; Ge, Z. On the Thermal Spalling Mechanism of Reactive Powder Concrete Exposed to High Temperature: Numerical and experimental studies. *Int. J. Heat Mass Transf.* **2016**, *98*, 493–507. [CrossRef]
54. Ju, Y.; Liu, H.; Liu, J.; Tian, K.; Wei, S.; Hao, S. Investigation on Thermophysical Properties of Reactive Powder Concrete. *Sci. China Technol. Sci.* **2011**, *54*, 3382–3403. [CrossRef]
55. Morsy, M.; Alsayed, S.; Aqel, M. Effect of Elevated Temperature on Mechanical Properties and Microstructure of Silica Flour Concrete. *Int. J. Civ. Environ. Eng.* **2010**, *10*, 1–6.
56. Abdulkareem, O.A.; Al Bakri, A.M.; Kamarudin, H.; Nizar, I.K.; Ala'eddin, A.S. Effects of Elevated Temperatures on the Thermal Behavior and Mechanical Performance of Fly Ash Geopolymer Paste, Mortar and Lightweight Concrete. *Constr. Build. Mater.* **2014**, *50*, 377–387. [CrossRef]
57. Su, H.; Xu, J.; Ren, W. Mechanical Properties of Geopolymer Concrete Exposed to Dynamic Compression under Elevated Temperatures. *Ceram. Int.* **2016**, *42*, 3888–3898. [CrossRef]
58. Mane, S.; Jadhav, H. Investigation of Geopolymer Mortar and Concrete under High Temperature. *Magnesium* **2012**, *2*, 384–390.
59. Pan, Z.; Sanjayan, J.G.; Rangan, B.V. An Investigation of the Mechanisms for Strength Gain or Loss of Geopolymer Mortar after Exposure to Elevated Temperature. *J. Mater. Sci.* **2009**, *44*, 1873–1880. [CrossRef]
60. Mendes, A.; Sanjayan, J.; Collins, F. Phase Transformations and Mechanical Strength of OPC/Slag Pastes Submitted to High Temperatures. *Mater. Struct.* **2008**, *41*, 345–350. [CrossRef]